

Crowd Counting with Online Knowledge Learning

Shengqin Jiang, Bowen Li, Fengna Cheng, Qingshan Liu, *Senior Member, IEEE*

Abstract—Efficient crowd counting models are urgently required for the applications in scenarios with limited computing resources, such as edge computing and mobile devices. A straightforward method to achieve this is knowledge distillation (KD), which involves using a trained teacher network to guide the training of a student network. However, this traditional two-phase training method can be time-consuming, particularly for large datasets, and it is also challenging for the student network to mimic the learning process of the teacher network. To overcome these challenges, we propose an online knowledge learning method for crowd counting. Our method builds an end-to-end training framework that integrates two independent networks into a single architecture, which consists of a shared shallow module, a teacher branch, and a student branch. This approach is more efficient than the two-stage training technique of traditional KD. Moreover, we propose a feature relation distillation method which allows the student branch to more effectively comprehend the evolution of inter-layer features by constructing a new inter-layer relationship matrix. It is combined with response distillation and feature internal distillation to enhance the transfer of mutually complementary information from the teacher branch to the student branch. Extensive experiments on four challenging crowd counting datasets demonstrate the effectiveness of our method which achieves comparable performance to state-of-the-art methods despite using far fewer parameters.

Index Terms—crowd counting; knowledge distillation; online training; feature relation

I. INTRODUCTION

CROWD Counting is a task that aims at automatically estimating the number of people in images or videos. It is a challenging task, as it involves dealing with varying densities, heavy occlusions, large scales, and complicated scenery. Due to its numerous practical applications, such as video surveillance, traffic management, and production forecasting, it has recently gained a lot of interest from both academia and industry.

Convolutional neural networks (CNNs) have demonstrated outstanding performance in visual tasks, leading to their widespread exploration in the field of crowd counting. Multi-column CNNs, as used in MCNN [1], have been employed to learn target density maps and handle varying crowd densities. However, these networks struggle to estimate high-density cases effectively. To overcome this limitation, Sindagi and Patel [2] proposed CP CNN, which leverages local and global contextual information for accurate crowd prediction. CSR-Net [3] used the first 10 layers as the front-end and dilated

Manuscript received *** **, 2023; revised *** **, 2023. (*Corresponding author: Qingshan Liu.*)

S. Jiang, B. Li and Q. Liu with the Jiangsu Key Lab of Big Data Analysis Technology (B-DAT), School of Computer, Nanjing University of Information Science and Technology, Nanjing 210044, China (e-mail: jiangshengqin@126.com; jslibowen@126.com; qslu@nuist.edu.cn)

F. Cheng is with College of Mechanical and Electronic Engineering, Nanjing Forestry University, Nanjing, 210037, China (e-mail: cfn1218@163.com)

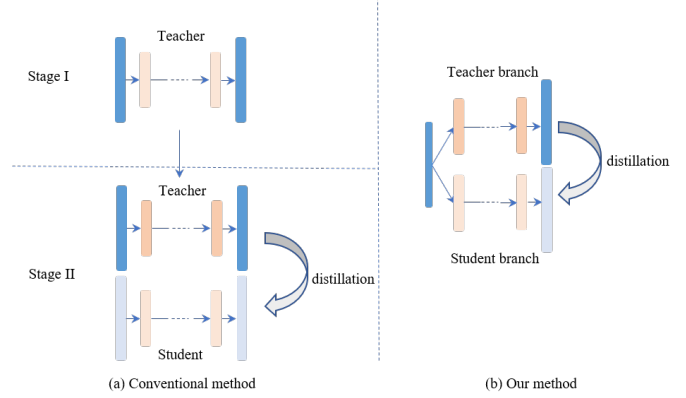


Fig. 1. Comparison of distillation pipeline (traditional method vs. our method). (a) The traditional method involves first training a teacher network, which is then followed by student network training; (b) Our method uses a distillation mechanism to jointly train teacher and student branches.

convolution layers as the back-end to learn scale variation. Recent models, such as SANet [4] and CAN [5], have incorporated some specific yet complicated structures to extract more powerful features. While these models offer performance benefits, they suffer from high computational complexity and long inference time. This makes them challenging to use in practical applications, such as edge computing and mobile terminals, where processing resources are limited.

Numerous strategies have been proposed to develop small yet efficient models with comparable performance to larger models, including pruning [6], [7] and quantization [8]. However, most of these methods require meticulous hyperparameter tuning or specialized hardware platforms [9], [10]. As an alternative, knowledge distillation (KD) makes use of supervised information from a superior-performing large model (teacher) to train a smaller model (student) [11]–[14], as shown in Fig. 1 (a). While this technique enhances the performance of the student model [9], [15], it also typically requires additional training time and may hinder the ability of the student model to truly master the learning process of the teacher model. Self-distillation is a potential solution to this problem, as it has been successfully applied to image classification [10], [16], [17]. However, applying it directly to high-density crowd counting tasks is challenging due to the difficulty in creating efficient soft targets for lightweight branching and achieving effective knowledge transfer.

To address the aforementioned challenges, we propose a solution in the form of an online knowledge learning network for crowd counting. This framework, depicted in Fig. 1 (b), is an end-to-end knowledge distillation approach, which avoids the need for two-phase training methods. It consists of a shared shallow module, a teacher branch, and a student

branch. The student branch employs approximately 1/4 of the channels of the teacher branch to reduce computational complexity. It is important to note that the pre-trained model initializes the shared shallow module and teacher branch to gain adequate domain-specific knowledge. To facilitate knowledge transfer between the two branches, we propose a feature relation distillation method. It enables the student branch to better understand the evolution of inter-layer features with the help of a newly constructed inter-layer relationship matrix. It complements response distillation as well as feature internal distillation in order to help the student branch out to understand the a prior knowledge of the teacher branch from a different perspective. We conduct experiments on several challenging datasets, demonstrating that our approach significantly improves the performance of the student branch. Specifically, the student branch surpasses the teacher branch on three large-scale datasets, achieving comparable results with some state-of-the-art methods.

- To the best of our knowledge, we at the first time propose an end-to-end online knowledge distillation framework for crowd counting, which can significantly reduce the training time, especially for large-scale datasets.
- We propose a new feature relation distillation method to assist the student branch in better understanding the evolution of inter-layer features by distilling the inter-layer relationship matrix from both branches.
- To effectively achieve knowledge transfer for this framework, three kinds of knowledge distillation are explored including feature internal distillation, feature relation distillation and response distillation.
- Extensive experiments on four benchmarks show the effectiveness of our framework. Moreover, our distilled model achieves comparable results to some state-of-the-art methods, despite having limited parameters.

II. RELATED WORKS

In this section, we will review some works related to our model. In what follows, the CNN-based crowd counting will be introduced first. Then we will go through some recent efforts on knowledge distillation.

A. Crowd Counting

The early methods for crowd counting relied on detection-based approaches, which applied object detection techniques to identify the entire person or head in the image and label the target with boxes to determine the final counting result. Although detection-based approaches perform well in sparse settings, they may result in significant counting inaccuracies in highly dense crowds.

To address this challenge, density-based methods have been introduced to reduce the difficulty of counting prediction. For instance, Zhang et al. [1] suggested generating a density map using Gaussian kernels for each input, which was then used for regression. This method has been shown to effectively mitigate the challenge of detecting densely populated regions, resulting in accurate crowd count prediction and density perception of its distribution. Following this, CSRNet [3] utilized dilated

convolution layers to expand the receptive field, resulting in a significant improvement in the prediction performance of the network. Several other approaches have been proposed to enhance network performance, including [20], [21], and [22]. However, these methods have more complex structural designs and heavier parameters, which could potentially impede efficient reasoning abilities.

B. Knowledge Distillation

Knowledge distillation (KD) is a compression technique that transfers the knowledge from a large pre-trained model to a compact model. Hinton et al. [11] first proposed to use the output of a well-trained model as the supervised signal to assist the training of student network. [23] utilized both the outputs and intermediate representations of teacher as cues to improve the performance of student. [24] proposed a noise-based regularization method to strengthen the robustness of student. SKT [9] exploited the structured knowledge of a well-optimized teacher to build a lightweight student. All of these strategies, however, go through the time-consuming two-phase training process. That is, before directing the learning of a student model, a high-capacity teacher model must be trained.

To sidestep this issue, online KD is put forward to distill the network itself [10], [16], [17]. [16] leverages the previous iteration's outputs as soft targets, but this risks increasing the mistake in the learning process, and deciding which iteration to use as a teacher is difficult. [13] proposed a self-distillation framework in which knowledge from the deeper layers can guide the learning of shallow layers. [17] put forwards a multi-step knowledge distillation by using a teacher assistant to bridge the gap between student and teacher networks. [10] built an improved soft targets for the intermediate output layers by top-down fusing feature maps from deep layers with a label generator. While these works do decrease the duration needed for two-phase knowledge distillation, they fail to consider the inter-feature information. Moreover, these studies solely address relatively straightforward classification tasks, rather than the more complex challenges of high-density prediction.

III. METHOD

In this section, we introduce our proposed online knowledge learning method for crowd counting, which uses a one-stage training paradigm and effectively transfers knowledge. As depicted in Fig. 2, the network framework comprises a teacher branch and a student branch. The teacher branch is rich in experience and can extract useful information from training data, while the student branch has fewer parameters and faster reasoning speed. We will begin by presenting our network architecture and then proceed to explain how we distill knowledge from the teacher branch to the student branch.

A. Network Architecture

Figure 2 illustrates the network structure, which is composed of a shared shallow module, a teacher branch, and a student branch. In particular, the input image is initially

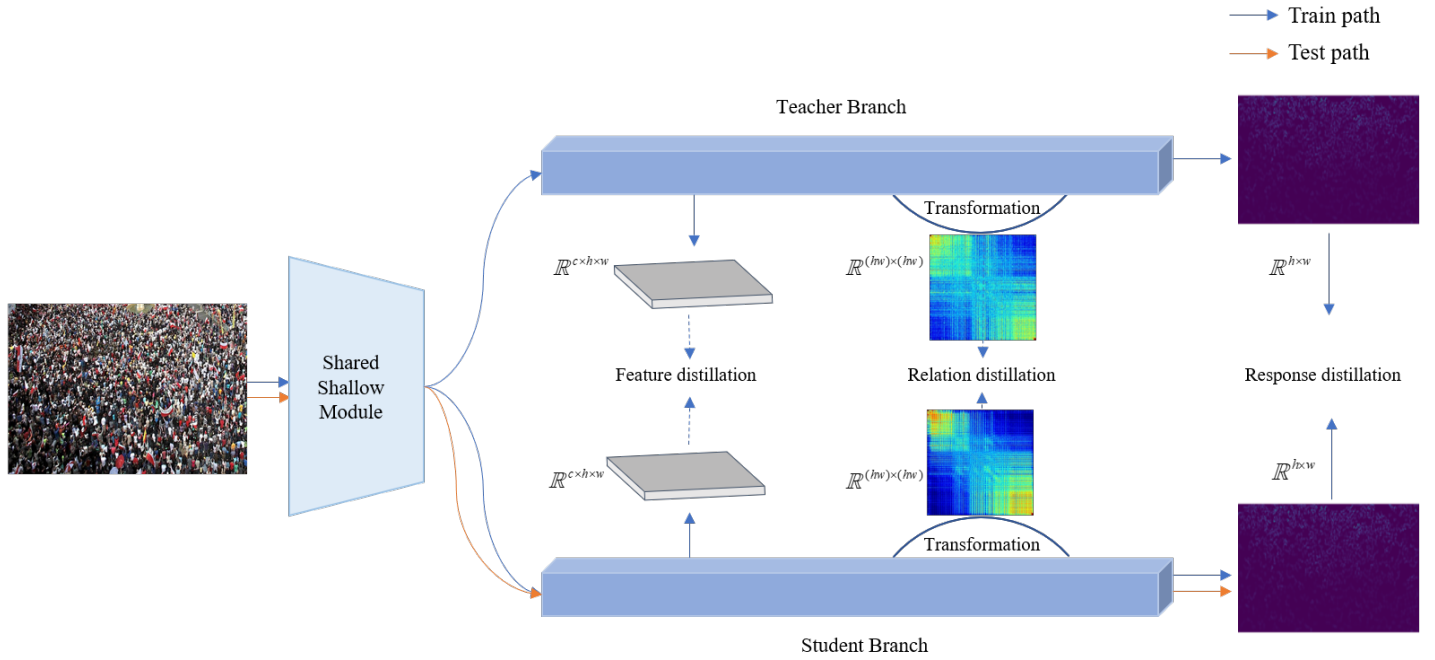


Fig. 2. An overview of the proposed online distillation network. It consists of shared shallow module, teacher branch and student branch. Meanwhile, feature distillation, relation distillation and response distillation are introduced to guide the knowledge learning from teacher branch to student branch.

processed by the shared shallow module to extract base features before being forwarded to the two branches. Both the teacher branch and the student branch output their own density maps, with the former serving as a mentor to the latter during training.

1) *Shared Shallow Module*: The early layers of 2D CNNs are commonly used to extract low-level features such as edges and corners. Here, we design a shared two-layer convolutional module for extracting spatial patterns. Specifically, we adopt the first two layers of VGG-16 [25] for this purpose, as they are effective and widely used in various tasks. This module consists of two 3×3 convolutions followed by max-pooling with a stride of (2, 2).

Since the teacher branch requires a lot of experience (please refer to the subsection III-A2 for details), the starting point of the module is to keep the network structure consistent with the shallow layer of the pre-trained model. In light of this, we initialize this module using the trained parameters. It is important to note that the shared module also serves as the initial layers of the student branch, so it should not have too many parameters. In other words, we should avoid introducing too many shallow layers in the teacher branch when designing the shared module.

2) *Teacher branch*: In addition to using the first two layers of VGG-16 in the shared shallow module, we employ the remaining layers of the first 10 layers of VGG-16 as the front-end of the teacher branch. This allows us to utilize the pre-trained model, which has strong transfer learning capabilities and a flexible design. The teacher branch is intended to act as an experienced mentor who can quickly learn new information and guide the student branch.

To improve the characterization capabilities of the teacher

branch further, we adopt a structure similar to CSRNet [3] by incorporating dilated convolutional layers in the back-end. This type of convolutional layers can directly enhance the network receptive field without increasing its parameters or computational complexity. Specifically, we use a light version of CSRNet consisting of 3 dilated convolutional layers.

3) *Student branch*: The channel capacity of a network is a critical factor that affects both inference speed and memory consumption. In our approach, we limit the number of channels in the teacher branch to approximately one-fourth of its original size to reduce the computational burden. However, following the design principle of VGG networks, reducing the number of channels directly to one-fourth may limit the network's ability to express shallow features.

To address this issue, we adopt a compromise method in which we keep the number of channels in the student branch constant until the first pooling layer. After that, we gradually reduce the number of channels in the remaining layers by one-fourth. Additionally, we can further reduce the number of channels by using multiples of one-fourth. This approach allows us to strike a balance between channel capacity and computational efficiency while maintaining the expressive power of the network.

B. Knowledge distillation

The limited number of channels in the student branch can hinder their ability to extract features effectively. Fortunately, knowledge distillation offers an effective strategy to mitigate this problem by providing additional supervision signals for knowledge transfer [11], [26]–[28]. To this end, we adopt three distillation techniques to enhance the learning capabilities of

the student branch: individual feature distillation, relation-in-relation distillation, and response distillation. Before delving into the details of these techniques, we introduce a feature grouping approach to better understand the proposed knowledge distillation strategy.

1) *Feature grouping*: In Fig. 2, an input image is first processed by the shared shallow module, which outputs a group of low-level features. These features are then fed into two separate branches with different channel capacities. Let us denote these features as $t_1(s_1)$ to represent the teacher (student) branch output. The feature map output by the i -th block in the teacher branch is denoted as t_i , where block partitioning begins from the convolution following the previous pooling operation to the next Max-Pooling. Similarly, the output of the i -th block in the student network is denoted as s_i . Formally, the features are grouped as follows:

$$T = \{t_2, t_3, t_4, t_5\}, S = \{s_2, s_3, s_4, s_5\}, \quad (1)$$

where T and S denote the feature sets of the teacher branch and the student branch, respectively.

The features cannot be distilled directly since the number of channels in the two branches is not aligned. Therefore, to maintain consistency in the feature dimensions, we apply a linear transformation function $f_{ad}(\cdot)$ to the output features of various blocks of the student network. This transformation function adapts s_i to s'_i , which has the same dimension as t_i . The transformation is defined as follows:

$$S' = f_{ad}(S) = \{s'_2, s'_3, s'_4, s'_5\}, \quad (2)$$

where S' is the feature groups transformed from S . It should be noted that this transformation is only employed during the training stage.

2) *Feature internal distillation*: Fine-grained semantic information is contained in multiple levels of features. Distilling features is a direct method for helping students express themselves in the same way as teacher do. To this end, we build a feature internal distillation method to minimize distribution similarity between s'_i and t_i . To achieve such a goal, mean square error (MSE) between features is a natural and simple choice. As the semantic structure of teacher and student branches differs, this choice may be overly tight, which will have a negative impact on the distillation. Moreover, our experiments show that this distillation method has poor compatibility with other types of distillation, not to mention its heavy calculation. Instead, we use a light metric, vector feature loss, to measure the similarity of s'_i and t_i . This metric not only reduces the redundant information between features, but also forms a complementary learning strategy with other methods. Concretely, we first feed both features s'_i and t_i into adaptive average pooling operation $p(\cdot) \in \mathbb{R}^{B \times C \times H \times W} \rightarrow \mathbb{R}^{B \times C \times 1 \times 1}$. Then the feature internal distillation is calculated by:

$$L_f = \sum_{i=2}^N \frac{1}{C_i} \|p(s'_i) - p(t_i)\|_2^2 \quad (3)$$

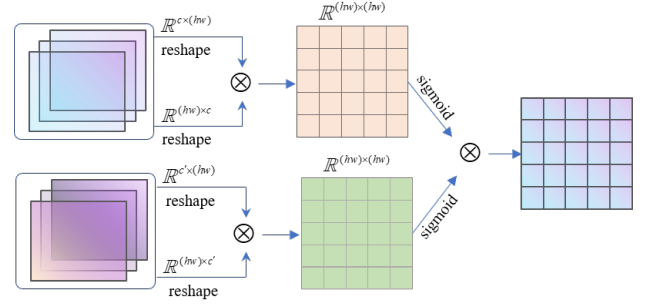


Fig. 3. Overview of feature relation module.

where C_i is the channel number of s'_i and t_i and N is the number of blocks.

3) *Feature relation distillation*: Semantic changes between layers reflect the evolution of features within the network, which is referred to as the inter-layer "flow" in [29]. Therefore, exploring the relationships between layers is crucial for helping student networks capture robust features. For example, [9] densely computes pairwise feature relationships using down-sampled block features. However, existing methods mainly focus on the relationship information of individual pixels and overlook the relationships between different pixels within the same layer. To address this issue, we propose a feature relationship module inspired by [30] that models the relationships between different pixels and the corresponding similarity between layers, after which a distillation strategy is used to help students branch out to learn the evolution of features between layers.

The overview of feature relation module is depicted in Fig. 3 to better explain the distillation process. Let us consider the teacher branch as an example. Firstly, we can obtain two feature maps $t_i \in \mathbb{R}^{B \times C_1 \times H \times W}$ and $t_j \in \mathbb{R}^{B \times C_2 \times H \times W}$ ($2 \leq i < j \leq N$) from different blocks. Next, we apply a reshape operation to transform the shape of the two feature maps, for example, for t_i , we obtain two new feature maps: $t_i^1 \in \mathbb{R}^{B \times (HW) \times C_1}$ and $t_i^2 \in \mathbb{R}^{B \times C_1 \times (HW)}$. Next, Multiply t_i^1 by t_i^2 , we obtain the correction matrix $K_i \in \mathbb{R}^{B \times HW \times HW}$ after sigmoid operation $g(\cdot)$. After the same operation, we have the correction matrix K_j for the feature map t_j as well. Finally, the relation matrix between the i -th and j -th block in the teacher branch is obtained, i.e., $R_{ij}^t = K_i \otimes K_j$. Formally, the inter-layer relationship matrix can be expressed as follows:

$$R_{ij}^t = \frac{g(t_i^1 \cdot t_i^2) \otimes g(t_j^1 \cdot t_j^2)}{H \cdot W} \quad (4)$$

where \otimes means element-wise product. After the same operation, we get the same relationship matrix of the student branch $R_{ij}^{s'}$ for the i -th and j -th block.

Here we simply use the L2 distance to measure the gap between two corresponding relationship. The feature relation loss is present as follows:

$$L_r = \sum_{2 \leq i < j \leq N} \|R_{ij}^{s'} - R_{ij}^t\|_2^2 \quad (5)$$

4) *Response distillation*: Recent work has revealed that response distillation is a type of learned label smoothing regularization [31]. In the traditional two-phase architecture, MSE is typically used as the loss function, but it is difficult to obtain comparable results in our distillation paradigm. We speculate that this is because it is challenging for the teacher branch to produce a strong output early in the training process, and therefore, response distillation based on MSE is not particularly strict, making it difficult to achieve effective regularization. Inspired by [32], we use SSIM loss as the response-based distillation loss, which is defined as follows:

$$L_s = 1 - SSIM(t_N, s'_N),$$

$$SSIM(t_N, s'_N) = \frac{(2\mu_{t_N}\mu_{s'_N} + c_1)(2\sigma_{t_N s'_N} + c_2)}{(\mu_{t_N}^2 + \mu_{s'_N}^2 + c_1)(\sigma_{t_N}^2 + \sigma_{s'_N}^2 + c_2)}, \quad (6)$$

where μ_x denotes the mean intensity of input x , σ_y denotes the standard deviation of input y , and σ_{xy} denotes the covariance of input x and y .

Finally, we perform knowledge distillation by minimizing the total loss as follows:

$$L = L_{st} + L_{tea} + \alpha_1 L_f + \alpha_2 L_r + \alpha_3 L_s \quad (7)$$

where L_{st} and L_{tea} are the MSE loss of student and teacher branches, α_1, α_2 and α_3 are tunable hyper-parameters to balance the loss terms.

IV. EXPERIMENT

In this part, we conduct comprehensive experiments on four challenging datasets to illustrate the effectiveness of our proposed strategy, including the ShanghaiTech dataset (Part A) [1] and UCF-QNRF [33], JHU-CROWD++ [34] and NWPU-Crowd [35]. We employ ShanghaiTech Part A to conduct ablation studies to demonstrate the efficiency of our suggested module and framework. Then, we compare our solution to other state-of-the-art methods on the four datasets.

A. Experiment Settings

All experiments in this study were implemented using PyTorch. Data augmentation is performed as follows: first, the image is randomly scaled to 0.8 to 1.2 times its original size. The scaled image is then randomly cropped into a 400×400 patch. Next, random flipping and gamma correction are applied. VGG-16 pretrained on ImageNet is used to initialize the first ten layers of the shared shallow module and the teacher branch. The remaining layers are initialized by a random Gaussian distribution with a standard deviation of 0.01. For training, the initial learning rate of the student branch is set to $1e^{-4}$, while that of the teacher branch is $1e^{-6}$. The same hyper-parameters settings ($\alpha_1 = 1, \alpha_2 = 10, \alpha_3 = 1000$) are adopted for all experiments. The network is trained for 600 epochs on ShanghaiTech Part-A and UCF-QNRF and 500 epochs on the remaining two datasets, using the Adam optimizer. The following subsection will introduce the four benchmarks mentioned.

B. Datasets

ShanghaiTech Part-A [1]: This dataset includes 482 images collected from the Internet, where 300 images are used for training and the rest for testing.

UCF-QNRF [33]: It is a challenging dataset, which contains 1,535 images collected from Internet with high-resolution. The annotated heads of samples range from 49 to 12,865, which has a huge variation of crowd density. There are 1,201 images for training and 334 images for testing.

JHU-CROWD++ [34]: This is a large scale unconstrained crowd counting dataset. It is collected under a variety of diverse scenarios and environmental conditions which contains 4,372 images with 1.51 million annotations. There are 2,772 images for training and 1600 images for testing.

NWPU-Crowd [35]: This is the largest crowd counting and localization benchmark. It contains various illumination scenes and has the largest density range from 0 to 20,033. It is made up of 1,525 images with a total of 1,251,642 label points. The average number of pedestrians per image is 815, with a high of 12,865. For most models, this configuration is a tremendous difficulty.

C. Ablation Study

In this part, we conduct an ablation study on the ShanghaiTech Part A dataset to assess the effectiveness of our proposed method, which we refer to as the Crowd Counting Distillation (CCD) Net for simplicity. As mentioned in [9], the number of channels is an important factor in balancing efficiency and accuracy in knowledge distillation. Therefore, we follow their approach and set the channel number of the student branch to be one-fourth of the teacher branch. We provide a detailed analysis of our ablation study in the following subsections

a) *Exploration on Online Knowledge Learning*: In this section, we present the results of our experiments to evaluate the effect of online knowledge learning. Table I shows the comparison between two-phase distillation and online distillation. Our proposed online distillation method outperforms the two-phase distillation method by a large margin, demonstrating the benefits of joint training. Specifically, online distillation achieved a performance gain of approximately 8% over the two-phase distillation method. Moreover, the online version is almost 1.4 times faster than the two-phase version, even with only 300 training samples. This indicates that the time discrepancy between the two methods becomes increasingly apparent as the sample size grows. For example, our online distillation method requires only 7310 minutes of training time for the NWPU-Crowd dataset.

Our proposed solution of online distillation, with only 0.67 times the parameters of the student network studied in SKT [9], is slightly better than the two-phase method (70.02 Vs. 71.55). These results demonstrate the efficacy of our distillation method as well as its high potential for knowledge transfer. Furthermore, our final solution with the pre-trained VGG model achieved significant performance improvement compared to the model without pre-trained VGG (70.2 Vs. 101.78). This demonstrates that the teacher branch with prior

TABLE I
COMPARISON OF TWO-PHASE DISTILLATION AND ONLINE DISTILLATION.

Method	MAE	Param (M)	Training Time (min)
SKT [9]	71.55	1.02	—
Two-phase Distillation (ours)	76.07	0.68	about 405
CCD Net w\o pre-trained VGG	101.78	0.68	—
CCD Net	70.02	0.68	about 280

TABLE II
ABLATION STUDY OF THE THREE KNOWLEDGE DISTILLATION MODULES.

Module	FID loss	FRD loss	RD loss	MAE
Baseline				92.45
	✓			92.61
		✓		74.43
			✓	72.69
	✓	✓		83.83
	✓		✓	75.22
		✓	✓	70.67
	✓	✓	✓	70.02

knowledge can better support the student branch to capture effective knowledge.

b) Exploration on Knowledge Distillation Configurations: To facilitate knowledge distillation, we adopt three modules: feature internal distillation (FID), feature relation distillation (FRD), and response distillation (RD). To evaluate the effectiveness of these modules, we establish a baseline, which is a student network consisting of the shared shallow module and the student branch, without knowledge distillation.

Table II summarizes the results of an ablation study on the three knowledge distillation modules. The results show that both FRD loss and RD loss significantly improve the performance of the student network compared to the baseline, indicating that they successfully transfer effective features. Moreover, the combination of these two losses further improves performance, with a MAE of 70.62. This suggests that these two modules are complementary to each other. However, FID loss seems to have little effect on knowledge transfer and achieves similar performance to the baseline. This indicates that the supervised signal provided by FID loss is weak when used alone. When combined with other losses, its performance varies. Interestingly, when paired with FRD loss and RD loss, the performance is marginally enhanced, and the MAE is increased by 0.65. We speculate that FRD and RD loss may be too stringent for knowledge transfer, and FID loss can effectively alleviate this issue. Next, we will evaluate the performance of each module separately.

Feature internal distillation Here, we go over the impact of feature internal distillation on the framework of this study in detail. To verify the benefit of our solution, we compare it to two commonly used metrics: MSE loss and Cos loss [9]. As shown in Table II, MSE and Cos losses are capable of fully transferring the knowledge stored at multiple layers, but KID loss is unable of doing so. This is mostly due to the fact that the KID only saves information between channels after a series of pooling operations, and the learned feature information is severely lost. It should be noted that the KID enjoys the benefits of less computation compared to the other two losses. As depicted in Table IV, it has good compatibility

TABLE III
COMPARISON OF FEATURE INTERNAL DISTILLATION LOSSES.

Loss	MAE
Baseline	92.45
+ MSE loss	77.97
+ Cos loss	76.52
+ FID loss	92.61

TABLE IV
COMPARISON OF FEATURE-LEVEL TRANSFER CONFIGURATION. ALL MODULES ARE USED, AND ONLY FEATURE LOSS IS CHANGED.

Transfer Configuration	MAE
W/O Feature Loss	70.67
+ MSE loss	71.78
+ Cos loss	70.76
+ FID loss	70.02

despite the poor performance of KID loss. As discussed above, we speculate that this is because MSE and COS loss can give a strong supervision signal for feature-level knowledge distillation, but they have a competing relationship with FRD loss and RD loss, making it difficult for the network to focus on effective feature learning.

Feature relation distillation To explore the information contained in features, we propose the relation distillation between features, which will capture the relationship between different pixels and different levels of features. There are two setups for our proposed FRD: sparse connected version (Sparse FRD) and densely connected version (FRD). FRD means that the elements in the feature sets (i.e., Eq. (1)) will be calculated for their corresponding relationships while Sparse RD only focuses on the relationship between adjacent elements. As shown in Table V, the performance of both versions has shown significant improvement, with FRD achieving the best MAE of 74.43. Notice that FSP loss [9] proposed for the inter-layer relation transfer only achieves a small amount of performance improvement. We attribute the weaker performance of the model to two factors. On the one hand, the FSP loss only considers the correlation of element pixels across different feature sets and overlooks the correlation of pixels within the features themselves. On the other hand, the correlation of the FSP loss in the original teacher network is fixed, while the features of the teacher branch in our network are dynamic, resulting in a weaker correlation established by the FSP.

Furthermore, Fig. 4 presents a visualization of the output of the FRD module, which is the relation matrix of different feature groups. The first row of the visualization shows that in low-level features, the relation matrix is decentralized, whereas in high-level features, the relation matrix is highly centralized.

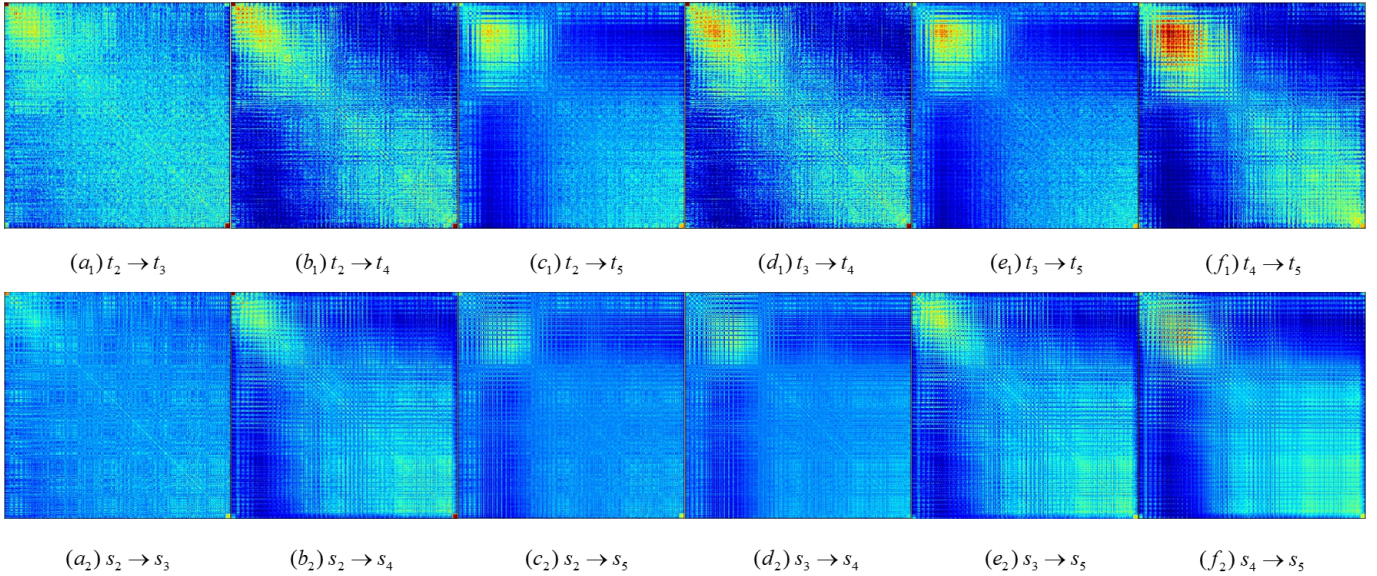


Fig. 4. Relation matrices of different feature groups. The relation matrix is produced by trained network on a test sample of ShanghaiTech Part A. The relationship matrix of the teacher and student branches is represented in the first and second rows, respectively. $t_i \rightarrow t_j$ ($s_i \rightarrow s_j$) denotes the relation matrix generated by $t_i(s_i)$ and $t_j(s_j)$. Brighter colors denote stronger relation values

TABLE V
COMPARISON OF FEATURE RELATION DISTILLATION LOSSES.

Loss	MAE
Baseline	92.45
+ FSP loss [9]	80.24
+ Cos loss	84.92
+ Sparse FRD loss	75.86
+ FRD loss	74.43

This can be attributed to the fact that low-level features contain detailed information such as edges, corners, and texture, leading to a significant degree of similarity between each pixel in the feature. On the other hand, high-level features extract extensive semantic information, resulting in significant variances between channels and various blocks. After distillation, we observe that the student branch approximates the relation matrix of the teacher branch while its distribution is more uniform compared to that of the teacher branch. This demonstrates that the FRD helps students in better understanding the differences between hierarchical features.

Response distillation Table VI presents a comparison of the response distillation losses, where we observe a significant improvement in the SSIM loss, achieving an MAE of 72.69 compared to the MSE loss. This improvement can be due to the fact that the SSIM loss evaluates the local pattern consistency of the output from both the teacher and student branches, whereas the MSE loss only evaluates the element pairwise similarity.

TABLE VI
COMPARISON OF RESPONSE DISTILLATION LOSSES.

Loss	MAE
Baseline	92.45
+ MSE Loss	86.68
+ SSIM Loss	72.69

D. Comparison with State-of-the-art Methods

To demonstrate the effectiveness of our method, we further compare CCD Net to some state-of-the-art crowd counting methods. Four datasets, i.e., ShanghaiTech Part-A, UCF-QNRF, JHU-Crowd++ and NWPU-Crowd are used for performance evaluation.

The final results are summarized in Tables VII, VIII, IX and X. As can be seen, our model performs admirably across all datasets with a small number of parameters. There are two findings on these datasets:

- Compared to training alone, the use of knowledge distillation in the student branch has resulted in significant improvements. The magnitude of this improvement becomes more pronounced with larger data collections. On the JHU-Crowd++ and NWPU-Crowd datasets, for example, the performance is more than or almost doubled.
- Interestingly, the student branch outperforms the teacher branch on three large-scale datasets, namely, UCF-QNRF, JHU-Crowd++, and NWPU-Crowd, while there is still a certain gap between the student branch and teacher branch on ShanghaiTech Part-A. This indicates that the network can be easily overfitted on a small dataset during the distillation step. Furthermore, we speculate that joint training indeed helps student networks better capture effective features, allowing it to outperform the teacher network.

Our findings suggest that our online training network is capable of effectively transferring knowledge. While we have achieved excellent performance, it is important to note that there is still a gap between our results and the latest benchmarks. For instance, the BL model outperforms ours by 12% on UCF-QNRF. The primary reason for this is due to the limited performance of our backbone. Therefore, in future work, we aim to enhance its applicability and further improve

its performance.

TABLE VII
COMPARISON OF CROWD COUNTING METHODS ON SHANGHAITECH PART-A.

Method	MAE	MSE
MCNN [1]	110.2	173.2
CP-CNN [2]	73.6	106.4
DNCL [36]	73.5	112.3
ACSCP [37]	75.7	102.7
L2R [38]	73.6	112.0
IG-CNN [39]	72.5	118.2
IC-CNN [40]	68.5	116.2
CFF [41]	65.2	109.4
SKT [9]	71.55	114.40
CSRNet	66.67	105.99
1/4 CSRNet	92.45	146.68
CCD Net	70.02	118.38

TABLE VIII
COMPARISON OF CROWD COUNTING METHODS ON UCF-QNRF.

Method	MAE	MSE
MCNN [1]	277	426
CMTL [42]	252	514
ResNet-101 [43]	190	277
CL [33]	132	191
TEDNet [44]	113	188
CANNet [5]	107	183
S-DCNet [45]	104.40	176.10
DSSINet [46]	99.10	159.20
CSRNet	145.54	233.32
1/4 CSRNet	186.31	287.65
CCD Net	136.26	240.83

TABLE IX
COMPARISON OF CROWD COUNTING METHODS ON JHU-CROWD++.

Method	MAE	MSE
MCNN [1]	188.9	483.4
CMTL [42]	157.8	490.4
DSSINet [46]	133.5	416.5
LSCCNN [47]	112.7	454.5
CANNet [5]	100.1	314.0
SANet [4]	91.1	320.4
BL [48]	75.0	299.9
CG-DRCN-CC-VGG16 [34]	82.3	328.0
CSRNet	85.9	309.2
1/4 CSRNet	182.86	539.00
CCD Net	85.51	315.71

TABLE X
COMPARISON OF CROWD COUNTING METHODS ON NWPU-CROWD.

Method	MAE	MSE
MCNN [1]	232.5	714.6
SANet [4]	190.6	491.4
C3F-VGG [49]	127.0	439.6
CANNet [5]	106.3	386.5
SCAR [50]	110.0	495.3
BL [48]	105.4	452.4
CSRNet	121.3	433.48
1/4 CSRNet	206.90	622.20
CCD Net	119.46	430.57

V. CONCLUSION

In this study, we propose an efficient online distillation network for crowd counting. Unlike the traditional two-

phase distillation technique, we introduce an end-to-end online knowledge distillation framework. The framework comprises three modules: a shared shallow module, a teacher branch, and a student branch, which integrate two traditionally distinct networks into a single trainable network. Then, we propose a new method for distilling feature relations, which enables the student branch to better understand the evolution of inter-layer features. This is achieved by constructing an inter-layer relationship matrix that captures the relationship between features across layers. It is integrated with response distillation and feature internal distillation methods to improve the transfer of mutually complementary information from the teacher branch to the student branch. Finally, our approach achieves comparable results to several state-of-the-art models, with significantly fewer parameters, as demonstrated through extensive experiments on four challenging datasets.

REFERENCES

- [1] Yingying Zhang, Desen Zhou, Siqin Chen, Shenghua Gao, and Yi Ma, "Single-image crowd counting via multi-column convolutional neural network," in *Proceedings of the IEEE Conference on Computer Vision and Pattern Recognition*, 2016, pp. 589–597. I, II-A, IV, IV-B, VII, VIII, IX, X
- [2] Vishwanath A Sindagi and Vishal M Patel, "Generating high-quality crowd density maps using contextual pyramid cnns," in *Proceedings of the IEEE International Conference on Computer Vision*, 2017, pp. 1861–1870. I, VII
- [3] Yuhong Li, Xiaofan Zhang, and Deming Chen, "Csrnet: Dilated convolutional neural networks for understanding the highly congested scenes," in *Proceedings of the IEEE/CVF Conference on Computer Vision and Pattern Recognition*, 2018, pp. 1091–1100. I, II-A, III-A2
- [4] Xinkun Cao, Zhipeng Wang, Yanyun Zhao, and Fei Su, "Scale aggregation network for accurate and efficient crowd counting," in *Proceedings of the European Conference on Computer Vision*, 2018, pp. 734–750. I, IX, X
- [5] Weizhe Liu, Mathieu Salzmann, and Pascal Fua, "Context-aware crowd counting," in *Proceedings of the IEEE/CVF Conference on Computer Vision and Pattern Recognition*, 2019, pp. 5099–5108. I, VIII, IX, X
- [6] Zhaowei Cai, Xiaodong He, Jian Sun, and Nuno Vasconcelos, "Deep learning with low precision by half-wave gaussian quantization," in *Proceedings of the Conference on Computer Vision and Pattern Recognition*, 2017, pp. 5918–5926. I
- [7] Yongming Rao, Jiwen Lu, Ji Lin, and Jie Zhou, "Runtime network routing for efficient image classification," *IEEE Transactions on Pattern Analysis and Machine Intelligence*, vol. 41, no. 10, pp. 2291–2304, 2018. I
- [8] Eunhyeok Park, Sungjoo Yoo, and Peter Vajda, "Value-aware quantization for training and inference of neural networks," in *Proceedings of the European Conference on Computer Vision*, 2018, pp. 580–595. I
- [9] Lingbo Liu, Jiaqi Chen, Hefeng Wu, Tianshui Chen, Guanbin Li, and Liang Lin, "Efficient crowd counting via structured knowledge transfer," in *Proceedings of the ACM International Conference on Multimedia*, 2020, pp. 2645–2654. I, II-B, III-B3, IV-C, IV-C0a, I, IV-C0b, IV-C0c, V, VII
- [10] Benlin Liu, Yongming Rao, Jiwen Lu, Jie Zhou, and Cho-Jui Hsieh, "Metadistiller: Network self-boosting via meta-learned top-down distillation," in *Proceedings of the European Conference on Computer Vision*, Springer, 2020, pp. 694–709. I, II-B, II-B
- [11] Geoffrey Hinton, Oriol Vinyals, Jeff Dean, et al., "Distilling the knowledge in a neural network," *arXiv preprint arXiv:1503.02531*, vol. 2, no. 7, 2015. I, II-B, III-B
- [12] Ying Zhang, Tao Xiang, Timothy M Hospedales, and Huchuan Lu, "Deep mutual learning," in *Proceedings of the IEEE Conference on Computer Vision and Pattern Recognition*, 2018, pp. 4320–4328. I
- [13] Linfeng Zhang, Jiebo Song, Anni Gao, Jingwei Chen, Chenglong Bao, and Kaisheng Ma, "Be your own teacher: Improve the performance of convolutional neural networks via self distillation," in *Proceedings of the IEEE/CVF International Conference on Computer Vision*, 2019, pp. 3713–3722. I, II-B

- [14] Yuenan Hou, Zheng Ma, Chunxiao Liu, and Chen Change Loy, "Learning lightweight lane detection cnns by self attention distillation," in *Proceedings of the IEEE/CVF International Conference on Computer Vision*, 2019, pp. 1013–1021. I
- [15] Xing Dai, Zeren Jiang, Zhao Wu, Yiping Bao, Zhicheng Wang, Si Liu, and Erjin Zhou, "General instance distillation for object detection," in *Proceedings of the IEEE/CVF Conference on Computer Vision and Pattern Recognition*, 2021, pp. 7842–7851. I
- [16] Chenglin Yang, Lingxi Xie, Chi Su, and Alan L Yuille, "Snapshot distillation: Teacher-student optimization in one generation," in *Proceedings of the IEEE/CVF Conference on Computer Vision and Pattern Recognition*, 2019, pp. 2859–2868. I, II-B, II-B
- [17] Seyed Iman Mirzadeh, Mehrdad Farajtabar, Ang Li, Nir Levine, Akihiro Matsukawa, and Hassan Ghasemzadeh, "Improved knowledge distillation via teacher assistant," in *Proceedings of the AAAI Conference on Artificial Intelligence*, 2020, vol. 34, pp. 5191–5198. I, II-B, II-B
- [18] Ross Girshick, "Fast r-cnn," in *Proceedings of the IEEE International Conference on Computer Vision*, 2015, pp. 1440–1448.
- [19] Joseph Redmon, Santosh Divvala, Ross Girshick, and Ali Farhadi, "You only look once: Unified, real-time object detection," in *Proceedings of the IEEE Conference on Computer Vision and Pattern Recognition*, 2016, pp. 779–788.
- [20] Shengqin Jiang, Xiaobo Lu, Yinjie Lei, and Lingqiao Liu, "Mask-aware networks for crowd counting," *IEEE Transactions on Circuits and Systems for Video Technology*, vol. 30, no. 9, pp. 3119–3129, 2019. II-A
- [21] Xiaoheng Jiang, Li Zhang, Mingliang Xu, Tianzhu Zhang, Pei Lv, Bing Zhou, Xin Yang, and Yanwei Pang, "Attention scaling for crowd counting," in *Proceedings of the IEEE/CVF Conference on Computer Vision and Pattern Recognition*, 2020, pp. 4706–4715. II-A
- [22] Yifan Yang, Guorong Li, Dawei Du, Qingming Huang, and Nicu Sebe, "Embedding perspective analysis into multi-column convolutional neural network for crowd counting," *IEEE Transactions on Image Processing*, vol. 30, pp. 1395–1407, 2020. II-A
- [23] Adriana Romero, Nicolas Ballas, Samira Ebrahimi Kahou, Antoine Chassang, Carlo Gatta, and Yoshua Bengio, "Fitnets: Hints for thin deep nets," *arXiv preprint arXiv:1412.6550*, 2014. II-B
- [24] Bharat Bhusan Sau and Vineeth N Balasubramanian, "Deep model compression: Distilling knowledge from noisy teachers," *arXiv preprint arXiv:1610.09650*, 2016. II-B
- [25] Karen Simonyan and Andrew Zisserman, "Very deep convolutional networks for large-scale image recognition," *arXiv preprint arXiv:1409.1556*, 2014. III-A1
- [26] Xiaojie Li, Jianlong Wu, Hongyu Fang, Yue Liao, Fei Wang, and Chen Qian, "Local correlation consistency for knowledge distillation," in *Proceedings of the European Conference on Computer Vision*. Springer, 2020, pp. 18–33. III-B
- [27] Jianping Gou, Baosheng Yu, Stephen J Maybank, and Dacheng Tao, "Knowledge distillation: A survey," *International Journal of Computer Vision*, vol. 129, no. 6, pp. 1789–1819, 2021. III-B
- [28] Byeongho Heo, Minsik Lee, Sangdoon Yun, and Jin Young Choi, "Knowledge transfer via distillation of activation boundaries formed by hidden neurons," in *Proceedings of the AAAI Conference on Artificial Intelligence*, 2019, vol. 33, pp. 3779–3787. III-B
- [29] Junho Yim, Donggyu Joo, Jihoon Bae, and Junmo Kim, "A gift from knowledge distillation: Fast optimization, network minimization and transfer learning," in *Proceedings of the IEEE Conference on Computer Vision and Pattern Recognition*, 2017, pp. 4133–4141. III-B3
- [30] Xiaolong Wang, Ross Girshick, Abhinav Gupta, and Kaiming He, "Non-local neural networks," in *Proceedings of the IEEE/CVF Conference on Computer Vision and Pattern Recognition*, 2018, pp. 7794–7803. III-B3
- [31] Li Yuan, Francis EH Tay, Guilin Li, Tao Wang, and Jiashi Feng, "Revisiting knowledge distillation via label smoothing regularization," in *Proceedings of the IEEE/CVF Conference on Computer Vision and Pattern Recognition*, 2020, pp. 3903–3911. III-B4
- [32] Zhou Wang, Alan C Bovik, Hamid R Sheikh, and Eero P Simoncelli, "Image quality assessment: from error visibility to structural similarity," *IEEE Transactions on Image Processing*, vol. 13, no. 4, pp. 600–612, 2004. III-B4
- [33] Haroon Idrees, Muhmmad Tayyab, Kishan Athrey, Dong Zhang, Somaya Al-Maadeed, Nasir Rajpoot, and Mubarak Shah, "Composition loss for counting, density map estimation and localization in dense crowds," in *Proceedings of the European Conference on Computer Vision*, 2018, pp. 532–546. IV, IV-B, VIII
- [34] Vishwanath Sindagi, Rajeev Yasarla, and Vishal MM Patel, "Jhu-crowd++: Large-scale crowd counting dataset and a benchmark method," *IEEE Transactions on Pattern Analysis and Machine Intelligence*, 2020. IV, IV-B, IX
- [35] Qi Wang, Junyu Gao, Wei Lin, and Xuelong Li, "Nwpu-crowd: A large-scale benchmark for crowd counting and localization," *IEEE Transactions on Pattern Analysis and Machine Intelligence*, vol. 43, no. 6, pp. 2141–2149, 2020. IV, IV-B
- [36] Zenglin Shi, Le Zhang, Yun Liu, Xiaofeng Cao, Yangdong Ye, Ming-Ming Cheng, and Guoyan Zheng, "Crowd counting with deep negative correlation learning," in *Proceedings of the IEEE/CVF Conference on Computer Vision and Pattern Recognition*, 2018, pp. 5382–5390. VII
- [37] Zan Shen, Yi Xu, Bingbing Ni, Minsi Wang, Jianguo Hu, and Xiaokang Yang, "Crowd counting via adversarial cross-scale consistency pursuit," in *Proceedings of the IEEE/CVF Conference on Computer Vision and Pattern Recognition*, 2018, pp. 5245–5254. VII
- [38] Xiaolei Liu, Joost Van De Weijer, and Andrew D Bagdanov, "Leveraging unlabeled data for crowd counting by learning to rank," in *Proceedings of the IEEE/CVF Conference on Computer Vision and Pattern Recognition*, 2018, pp. 7661–7669. VII
- [39] Deepak Babu Sam, Neeraj N Sajjan, R Venkatesh Babu, and Mukundhan Srinivasan, "Divide and grow: Capturing huge diversity in crowd images with incrementally growing cnn," in *Proceedings of the IEEE/CVF Conference on Computer Vision and Pattern Recognition*, 2018, pp. 3618–3626. VII
- [40] Viresh Ranjan, Hieu Le, and Minh Hoai, "Iterative crowd counting," in *Proceedings of the European Conference on Computer Vision*, 2018, pp. 270–285. VII
- [41] Zenglin Shi, Pascal Mettes, and Cees GM Snoek, "Counting with focus for free," in *Proceedings of the IEEE/CVF International Conference on Computer Vision*, 2019, pp. 4200–4209. VII
- [42] Vishwanath A Sindagi and Vishal M Patel, "Cnn-based cascaded multi-task learning of high-level prior and density estimation for crowd counting," in *Proceedings of the IEEE International Conference on Advanced Video and Signal Based Surveillance*. IEEE, 2017, pp. 1–6. VIII, IX
- [43] Kaiming He, Xiangyu Zhang, Shaoqing Ren, and Jian Sun, "Deep residual learning for image recognition," in *Proceedings of the IEEE Conference on Computer Vision and Pattern Recognition*, 2016, pp. 770–778. VIII
- [44] Xiaolong Jiang, Zehao Xiao, Baochang Zhang, Xiantong Zhen, Xianbin Cao, David Doermann, and Ling Shao, "Crowd counting and density estimation by trellis encoder-decoder networks," in *Proceedings of the IEEE/CVF Conference on Computer Vision and Pattern Recognition*, 2019, pp. 6133–6142. VIII
- [45] Haipeng Xiong, Hao Lu, Chengxin Liu, Liang Liu, Zhiguo Cao, and Chunhua Shen, "From open set to closed set: Counting objects by spatial divide-and-conquer," in *Proceedings of the IEEE/CVF International Conference on Computer Vision*, 2019, pp. 8362–8371. VIII
- [46] Lingbo Liu, Zhilin Qiu, Guanbin Li, Shufan Liu, Wanli Ouyang, and Liang Lin, "Crowd counting with deep structured scale integration network," in *Proceedings of the IEEE/CVF International Conference on Computer Vision*, 2019, pp. 1774–1783. VIII, IX
- [47] Deepak Babu Sam, Skand Vishwanath Peri, Mukuntha Narayanan Sundaraman, Amogh Kamath, and R Venkatesh Babu, "Locate, size, and count: accurately resolving people in dense crowds via detection," *IEEE Transactions on Pattern Analysis and Machine Intelligence*, vol. 43, no. 8, pp. 2739–2751, 2020. IX
- [48] Zhiheng Ma, Xing Wei, Xiaopeng Hong, and Yihong Gong, "Bayesian loss for crowd count estimation with point supervision," in *Proceedings of the IEEE/CVF International Conference on Computer Vision*, 2019, pp. 6142–6151. IX, X
- [49] Junyu Gao, Wei Lin, Bin Zhao, Dong Wang, Chenyu Gao, and Jun Wen, "C³ framework: An open-source pytorch code for crowd counting," *arXiv preprint arXiv:1907.02724*, 2019. X
- [50] Junyu Gao, Qi Wang, and Yuan Yuan, "Scar: Spatial-/channel-wise attention regression networks for crowd counting," *Neurocomputing*, vol. 363, pp. 1–8, 2019. X